



## Osteoprotective effects of the neuropeptide VIP: insights from triple cultures of human osteocytes, osteoblasts, and osteoclasts

David Castro-Vázquez<sup>a</sup>, Iván García-López<sup>a</sup>, Katharina Wirsig<sup>c</sup>, Paula Arribas-Castaño<sup>a</sup>, Rosa P. Gomariz<sup>a</sup>, Carmen Martínez<sup>b,d</sup>, Yasmina Juarranz<sup>a,d,1</sup>, Anne Bernhardt<sup>c,1</sup>, Mar Carrión<sup>a,d,1,\*</sup>

<sup>a</sup> Complutense University of Madrid, Department of Cell Biology and Histology, Faculty of Biological Sciences, 28040 Madrid, Spain

<sup>b</sup> Complutense University of Madrid, Departmental Section of Cell Biology and Histology, Faculty of Medicine, 28040 Madrid, Spain

<sup>c</sup> Centre for Translational Bone, Joint and Soft Tissue Research, University Hospital Carl Gustav Carus and Faculty of Medicine, Technische Universität Dresden, Germany

<sup>d</sup> Musculoskeletal Pathology Group, San Carlos Clinical Hospital, San Carlos Health Research Institute (IdISSC), Madrid, Spain

### ARTICLE INFO

#### Keywords:

VIP  
Osteocyte differentiation  
*In vitro* bone model  
Sclerostin  
RANKL/OPG ratio

### ABSTRACT

Bone remodelling is a dynamic process of osteoblastic bone formation and osteoclastic bone resorption, regulated by local, paracrine and endocrine factors, in which osteocytes act as orchestrators of bone homeostasis. Among these regulatory factors, the neuropeptide VIP (vasoactive intestinal peptide) has demonstrated osteoprotective effects by inhibiting osteoclastogenesis and promoting osteoblast differentiation. However, its potential role in osteocyte biology remains unexplored. In this study, we investigated the effect of VIP on the differentiation of primary human osteocytes. We describe for the first time the expression of VIP and its receptors during *in vitro* osteocyte differentiation. Our results show that VIP promotes osteocytogenesis, accompanied by a reduction in the RANKL/OPG ratio, thereby supporting its role as an anti-osteoclastogenic factor. To better mimic the complexity of bone tissue, we performed triple co-cultures of osteoblasts and simultaneously differentiating osteocytes and osteoclasts, in the presence or absence of VIP. Our results confirmed that VIP supports the osteoblast-to-osteocyte transition and promotes an osteoprotective phenotype, characterized by a reduced RANKL/OPG ratio and decreased *SOST* expression. The downregulation of sclerostin may attenuate osteocyte-mediated inhibitory signalling toward osteoblasts and, in turn, contribute to the reduction of the osteoblastic RANKL/OPG ratio. Collectively, our findings reinforce the anti-osteoclastogenic actions of VIP, supporting its role as a potential osteoprotective factor.

### Introduction

Bone remodelling is a complex physiological process essential for maintenance of the bone structure, its adaptation to mechanical demands and the repair of skeletal damage. It depends on the tightly coordinated activity of osteoclasts, which degrade old or damaged bone, and osteoblasts, responsible for the production of new bone restoring tissue integrity and strength.<sup>1,2</sup> The dynamic interplay between these cells is regulated at multiple levels, including local cytokines and growth factors, systemic hormones, and neural signalling molecules. Osteocytes play a central role in this process, acting as mechanosensors and endocrine regulators.<sup>3–5</sup>

Osteocytes, the most abundant cells in adult bone, represent

terminally differentiated cells of the osteoblast lineage that become surrounded by the newly mineralizing bone matrix. During transition from osteoblasts to osteocytes, termed osteocytogenesis, cells down-regulate osteoblastic markers related to mineralizing activity such as alkaline phosphatase and osteocalcin, encoded by *ALPL* and *BGLAP* respectively, while upregulating osteocyte-specific genes including *SOST* and *MEPE*, which encode sclerostin and matrix extracellular phosphoglycoprotein.<sup>6,7</sup> Simultaneously, their morphology evolves from a polygonal to a stellate shape, with extensive cytoskeletal remodelling. The formation of dendritic processes leads to their integration into the lacuno-canalicular network connecting neighbouring osteocytes as well as other effector cells in the bone. This structural adaptation is crucial for sensing mechanical and hormonal stimuli,

\* Corresponding author at: Complutense University of Madrid, Department of Cell Biology and Histology, Faculty of Biological Sciences, 28040 Madrid, Spain.  
E-mail address: [macarrio@ucm.es](mailto:macarrio@ucm.es) (M. Carrión).

<sup>1</sup> These authors jointly supervised this work: Yasmina Juarranz, Anne Bernhardt and Mar Carrión.

allowing osteocytes to orchestrate bone homeostasis via paracrine signalling to osteoclasts and osteoblasts.<sup>5,8</sup>

Mature osteocytes are characterized by the expression of *SOST*, the gene that encodes the protein sclerostin, which inhibits osteoblast function and suppresses bone formation.<sup>8</sup> As regulators of bone resorption, osteocytes are also the main source of the receptor activator of nuclear factor kappa-B ligand (RANKL) responsible for driving the process of osteoclast differentiation and activation, known as osteoclastogenesis.<sup>9,10</sup> RANKL is a cytokine of the tumour necrosis factor superfamily, which is additionally synthesized by bone marrow-derived stromal cells, osteoblasts and activated T lymphocytes.<sup>11</sup> The interaction between RANKL and its receptor RANK on the surface of osteoclast precursors represents a critical step for activating the nuclear factor of activated T-cells cytoplasmic 1 (NFATc1). This transcriptional factor is recognized as a master regulator for osteoclastogenesis, promoting the expression of genes such as dendritic cell-specific transmembrane protein (DC-STAMP), essential for osteoclast multinucleation, as well as tartrate-resistant acid phosphatase (TRAP) and cathepsin K, both critical enzymes for bone resorption activity.<sup>12,13</sup> On the other hand, RANKL induced osteoclastogenesis can be neutralized by the presence of osteoprotegerin (OPG), a decoy receptor frequently released by RANKL-expressing cells, including both osteoblasts and osteocytes. Under physiological conditions, the RANKL/OPG ratio represents a key index of bone resorption and osteoclastogenesis, acting as a crucial determinant of bone mass.<sup>14</sup>

Concomitantly, growing evidence indicates that bone homeostasis is tightly regulated by neural signalling networks. Notably, a wide range of bioactive neuropeptides contribute to the coordinated activity of bone cells through their specific receptors expressed within the bone micro-environment.<sup>3,4</sup> Among these, vasoactive intestinal peptide (VIP) has been identified as a bone homeostatic mediator, exerting its effects mainly through VPAC1 and VPAC2 receptors.<sup>15</sup> Compelling findings from animal models and *in vitro* studies using human and murine cells indicate that VIP inhibits osteoclastogenesis by directly impairing osteoclast differentiation and resorptive activity, and indirectly through a negative modulation of the RANKL/OPG ratio.<sup>16–22</sup> Evidence from *in vivo* studies consistently demonstrates that VIP reduces bone erosion in experimental models of rheumatoid arthritis<sup>23,24</sup> and is associated with a slower rate of bone density decline in early arthritis patients,<sup>16</sup> while also inhibiting alveolar bone loss in rat models of periodontitis.<sup>25</sup> Furthermore, VIP has been shown to stimulate osteogenic differentiation of rat and human bone marrow-derived mesenchymal stem cells (BM-MSCs).<sup>26,27</sup> In addition, VIP enhanced bone repair *in vivo*, promoting healing in rat skull defect models and accelerating fracture recovery in chemically sympathectomized mice.<sup>26,28</sup>

In line with its proposed role in neuro-osteogenic interactions, VIP has been detected in the bone marrow, the epiphyseal growth plate, and periosteal nerve fibres.<sup>21,29</sup> Notably, its expression is not restricted to physiological conditions, as VIP has also been identified in subchondral bone, bone marrow cavities, and osteocyte-like cells of patients with osteoarthritis.<sup>30,31</sup> Furthermore, beyond its neuronal origin, VIP is also produced by immune and endocrine cells,<sup>32</sup> and more recently, its expression has been demonstrated in human osteoblasts differentiated *in vitro*,<sup>27</sup> suggesting a potential autocrine role within the bone microenvironment.

Despite accumulating evidence positioning VIP as a neuropeptide critically involved in regulating the cellular mechanisms underlying bone homeostasis, and the well-established role of osteocytes as pivotal mediators of bone turnover, the effect of VIP on osteocytogenesis and on osteocyte biology remain largely unexplored to date. Furthermore, the influence of this neuropeptide on the reciprocal interactions among bone cells responsible for bone remodelling has yet to be elucidated. In this context, a 3D *in vitro* model of osteocyte differentiation<sup>33</sup> and a recently established triple co-culture system comprising primary human osteoblasts and precursors of both osteocytes and osteoclasts<sup>34</sup> was used to investigate the effects of VIP exposure on the involved cell types

completing its characterization as a neuroimmunological-osteogenic mediator with osteoprotective effects.

## Materials and methods

### Cell culture

#### Sources of osteoblasts/osteocytes and osteoclasts

Osteoblast precursors were isolated from human femoral heads of patients who had undergone total hip replacement surgery at the University Hospital Carl Gustav Carus Dresden (Germany) as described in.<sup>33</sup> Samples were obtained from 7 donors with ages ranging from 55 to 75 years (Table 1). The precursors were cultured in the expansion medium ( $\alpha$ -MEM, 10 % FCS and 1 % P/S), until passage 4 was reached. Then, the cells were cultured for 7 days in osteogenic medium [ $\alpha$ -MEM, 10 % FCS, 1 % P/S, 10 mM  $\beta$ -GP, 50  $\mu$ M AAP and 10<sup>-7</sup> M dexamethasone] to obtain mature osteoblasts.

Osteoclasts were differentiated from PBMC, which were isolated from four samples of leuco-platelet concentrate obtained from the German Red Cross, Dresden. Information on sex and age of the blood donors was not provided by the German Red Cross. PBMCs were isolated by density gradient centrifugation, followed by lysing of erythrocytes. For monocyte isolation by adherence, PBMCs were seeded in 24-well plates at 1·10<sup>6</sup> cells/well in  $\alpha$ -MEM supplemented with 10 % hi-FCS, 1 % P/S and 25 ng/mL M-CSF (macrophage colony stimulating factor) and maintained at 37°C in an incubator for 3 days (Fig. 1).

#### Osteoblasts and differentiation of osteocytes

For osteocyte differentiation, human pre-osteoblasts from 7 donors were harvested with Trypsin/EDTA 1X following expansion in  $\alpha$ -MEM with 10 % FCS and 1 % penicillin/streptomycin (P/S). After osteogenic differentiation for 7 days (expansion medium supplemented with 10<sup>-7</sup> M dexamethasone (Dex), 10 mM  $\beta$ -glycerophosphate ( $\beta$ -GP) and 12.5  $\mu$ g/mL ascorbic acid-2-phosphate (AAP), all osteogenic supplements from Sigma-Aldrich), pre-differentiated osteoblasts were embedded in collagen gels based on the protocol described by Bernhardt et al.<sup>35</sup> Briefly, collagen gels were prepared by mixing 8 parts of collagen solution [3 mg/mL rat tail type I collagen (Meidrix)] with 1 part of HBSS 10X (PAN-Biotech GmbH) with phenol red as pH indicator and 1 M NaOH to adjust the pH of the mixture to physiological conditions. Osteoblasts were resuspended in this mixture at a final concentration of 1·10<sup>5</sup> cells/mL, and 500  $\mu$ L of this suspension was added to 24-well plates. Subsequently, gels were allowed to solidify at 37°C for 30

**Table 1**

Donor information for primary human cells, which were used for the differentiation of osteoblasts, osteocytes and osteoclasts in seven independent experiments for monoculture and seven independent experiments for triple culture.

Monoculture		
Experiment no.	Osteoblasts/osteocytes	
1	female 75 years	
2	female 56 years	
3	female 58 years	
4	male 65 years	
5	male 57 years	
6	male 55 years	
7	male 62 years	
Triple culture		
Experiment no.	Osteoblasts/osteocytes	Osteoclasts
1	female 56 years	PBMC donor 1
2	male 62 years	PBMC donor 2
3	male 65 years	PBMC donor 2
4	female 55 years	PBMC donor 3
5	male 57 years	PBMC donor 3
6	female 55 years	PBMC donor 4
7	male 57 years	PBMC donor 4

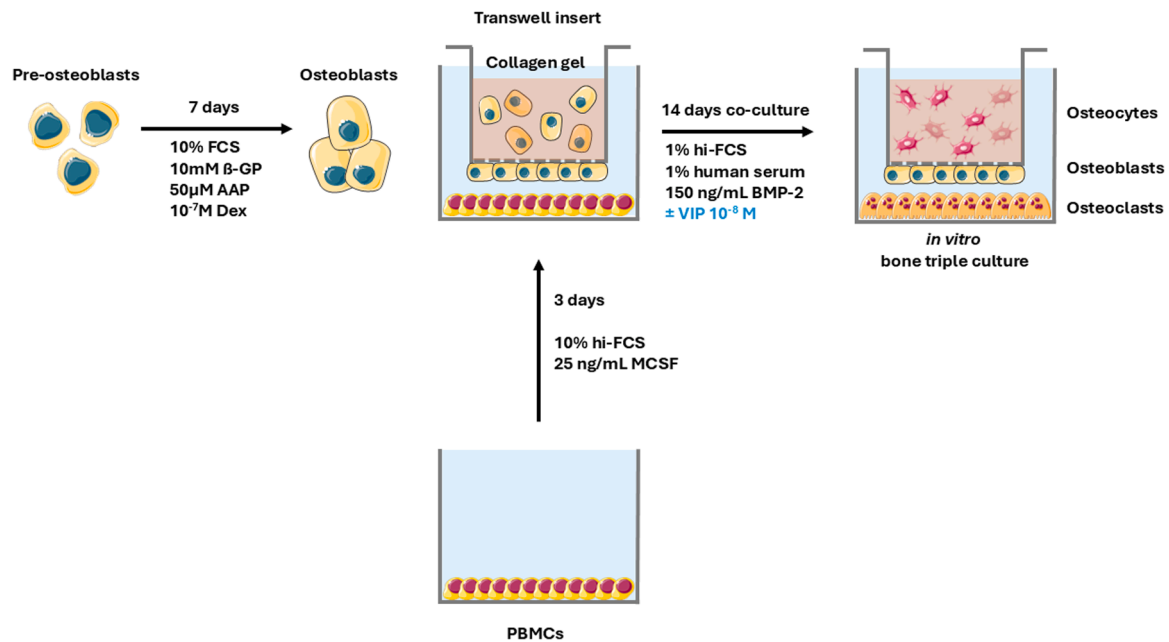


**Fig. 1.** Diagram of the experimental design used to establish *in vitro* triple cultures of osteoblasts and simultaneously differentiating osteocytes and osteoclasts derived from freshly isolated PBMCs.  $\beta$ -glycerophosphate ( $\beta$ -GP), ascorbic acid-2-phosphate (AAP), dexamethasone (Dex), heat inactivated FCS (hi-FCS), bone morphogenetic protein 2 (BMP-2), macrophage colony stimulating factor (MCSF), vasoactive intestinal peptide (VIP).

minutes. After collagen gelation, 500  $\mu$ L of monoculture medium consisting of  $\alpha$ -MEM, 2 % fetal calf serum (FCS), 1 % P/S, 10 mM  $\beta$ -GP, 50  $\mu$ M AAP and 100 ng/mL bone morphogenetic protein-2 (BMP2) were added to each well. Besides this control group, VIP  $10^{-8}$  M was added to test its impact on osteocyte differentiation. Osteocyte monocultures in the presence and absence of the neuropeptide were maintained for 14 days at 37°C in a humidified atmosphere containing 5 % CO<sub>2</sub>, with a complete medium change on day 7 and VIP added every 3-4 days to maintain a stable concentration.

#### Triple co-cultures with osteoblasts and simultaneously differentiating osteocytes and osteoclasts from their respective precursors

*In vitro* bone triple co-cultures of collagen hydrogel-embedded osteoblasts (differentiating to osteocytes), osteoblasts and PBMCs (differentiating to osteoclasts) were performed in transwell inserts (0.4  $\mu$ m pore size, TC Inserts Sarstedt) in 24-well plates as previously published<sup>34</sup> (Fig. 1). A total of seven independent triple co-cultures were established under these conditions (Table 1).

These transwell constructs consisted of primary human osteoblasts predifferentiated in osteogenic medium and embedded in 250  $\mu$ L collagen gel matrix at a final concentration of  $1 \cdot 10^5$  cells/mL on the basal side of the transwell inserts. Once the gels were solidified, the transwell inserts were inverted to allow seeding of osteoblasts on the apical side of the membrane. Osteoblasts were then seeded at a density of  $5 \cdot 10^4$  cells on the apical surface of the transwell membrane. Cells were allowed to attach to the membrane for 3 h in the incubator at 37°C (Supplementary Figure 1). Afterwards, the constructs were placed in 24-well plates pre-seeded with PBMCs ( $10^6$  cells per well, see 1.1).

After the triple co-cultures were built up, medium that supports both osteocyte-differentiation and osteoclast-formation ( $\alpha$ -MEM + 1 % heat inactivated FCS (hi-FCS) + 1 % human serum + 1 % P/S + 100 ng/mL BMP2) was added to the constructs in substitution of monoculture culture medium. Besides, triple co-cultures were conducted in the presence or absence of VIP  $10^{-8}$ M. and maintained for 14 days (Fig. 1). Culture medium was replaced on day 7 and VIP was added every 3-4 days to keep a stable concentration.

#### Fluorescence microscopy

Immunofluorescence studies were performed to visualize F-actin in osteocytes, osteoblasts and osteoclasts. Osteocyte-containing collagen gels were removed from wells (monocultures) or inserts (triple co-cultures). The samples were washed with PBS, fixed with 4 % paraformaldehyde for 1 h, permeabilized with 0.1 % TritonX-100 in PBS for 15 min and then blocked with 5 % bovine serum albumin (BSA) in PBS for 1 hour. Once blocked, the samples were incubated overnight at 4 °C with Phalloidin-iFluor 488 (1:1000; Abcam) to visualize the cytoskeleton and DAPI (1:1000) to stain nuclei. Images were captured using an Olympus Fluoview-1200 and, additional images included as supplementary data obtained with a Keyence BZ-X810. All images were processed with ImageJ.

#### RNA isolation, cDNA synthesis and PCR

For gene expression analysis, RNA was isolated from osteocytes, osteoblasts or osteoclasts. Osteocyte-containing collagen gels from monocultures and triple co-cultures were removed from the wells or the inserts, respectively, and digested for RNA isolation. Gels were incubated in a collagenase II solution (3 mg/mL in  $\alpha$ -MEM, supplemented with 1 % P/S, 10 % FCS and 3 mM CaCl<sub>2</sub>) for 1 h at 37 °C with orbital shaking. The samples were then centrifuged at 1500 rpm for 5 min, washed with PBS and centrifuged again to obtain an osteocyte pellet.

For the triple co-cultures, membranes with osteoblasts were separated from the transwell inserts using surgical tweezers. Total RNA was isolated using the commercially available peqGOLD MicroSpin Total RNA Kit (Peqlab). RNA was quantified using Nanodrop, and cDNA synthesis was performed using the High-Capacity cDNA Reverse Transcription Kit (Life Technologies).

Specific TaqMan gene expression assays for target genes (*ALPL*, *BGLAP*, *SOST*, *MEPE*, *DCSTAMP*, *NFATC1*, *CTSK*, *ACP5*, *TNFSF11*, *TNFRSF11B*, *VIPR1* and *VIPR2*) and *ACTB* as housekeeping gene were used along with TaqMan Fast Advanced Master Mix (Applied Biosystems) to perform real-time qPCR analysis. PCR was run with an Applied Biosystems 7500 fast Real-Time PCR system. Assays were made in triplicate and gene expression results were normalized to the

expression levels of *ACTB*.

The VIP gene was amplified by means of conventional PCR (Bio-tools). The sequence of primers used for human *VIP* (NM\_003381.4) was forward, 5'-ACGCTACTCAGATGCAGTCTTCAC-3'; and reverse, 5'-TCGTCCTCTTCCATTGAGAATT-3'. The PCR products were analysed in agarose gels, purified with the Qiagen PCR purification Kit and the correct size and sequence of the amplified products were checked through Sanger sequencing.

#### Western blot for VIP receptors VPAC1 and VPAC2

As described in the RNA isolation section, osteocytes were isolated from collagen gels using a digestion step with collagenase II. Then, the protein extracts were obtained using ice-cold radioimmunoprecipitation assay buffer (ThermoFisher). Total protein was quantified using the commercial Pierce BCA Protein Assay Kit (ThermoFisher). 50 µg of total protein from each sample was used for VIP receptor immunodetection experiments. Protein separation was performed by 10 % sodium dodecyl sulfate–polyacrylamide gel electrophoresis (SDS–PAGE) under denaturing conditions and then transferred to polyvinylidene difluoride (PVDF) membranes. After blocking, membranes were incubated o/n at 4°C with the following primary antibodies: mouse monoclonal anti-human VPAC2 (1:1000; Abnova), rabbit polyclonal anti-human VPAC1 (1:10000; ThermoFisher) and rabbit anti-human GAPDH (1:10000; Sigma) as a loading control. Then, horseradish peroxidase (HRP)-conjugated secondary antibodies (Amersham ECL) were used: anti-mouse (1:5000) and anti-rabbit (1:10000 for VPAC1 and 1:15000 for GAPDH). Proteins were detected using SuperSignal WestPico PLUS (ThermoFisher). Results were photographed with Bio-Rad Gel Doc XR+ System.

#### Immunohistochemistry of VIP in human compact bone sections

Trabecular bone fragments (50 mm) were isolated from the femoral heads, fixed overnight with 4 % PFA in PBS, decalcified using Osteosoft solution (Merck) for 12 weeks, embedded in paraffin, and sectioned at 3 µm thickness. Sections were incubated in citrate buffer (10 mM sodium citrate, 0.05 % Tween-20 pH 6) at 60°C for 1 h. After antigen retrieval, the endogenous peroxidase was blocked by incubation with 3 % H<sub>2</sub>O<sub>2</sub> in methanol for 10 min. The samples were blocked with 5 % BSA in PBS for 1 h and then incubated with the primary rabbit anti-human VIP antibody (1:100 in PBS-BSA 2 %; Sigma), overnight at 4°C. Sections incubated with 2 % PBS-BSA were used as a secondary antibody control. Slides were then incubated for 35 min with HRP-conjugated anti-rabbit secondary antibody (1:100 in PBS-BSA 2 %; ECL). Staining was visualized with diaminobenzidine (DAB), and samples were counterstained with 1 % alcian blue and 2 % light green in distilled H<sub>2</sub>O - acetic acid 3 % and 2 %, respectively.

#### Statistical analysis

Data were analysed using GraphPad Prism 8.0 software. All data sets were first subjected to outlier detection using the ROUT method ( $Q = 1$  %), and subsequent statistical analyses were performed on the remaining values. Parametric variables were analysed via t-test, while non-parametric variables were analysed using Mann-Whitney U test. Welch's correction was also applied when variances of the analysed groups were different. Two-sided p-values <0.05 were considered significant (\* $p < 0.05$ ; \*\* $p < 0.01$ ; \*\*\* $p < 0.001$ ).

## Results

#### Characterizing the VIP/receptor axis in human osteocytes

Based on our previous findings demonstrating the expression of VIP and its specific receptors in human osteoblasts, we first assessed whether

this signalling system is maintained in human osteocytes after their differentiation from osteoblasts.

VIP gene expression was detected by conventional PCR in all samples of human osteocytes differentiated in 3D collagen gels. The identity of the PCR products was confirmed by electrophoretic analysis followed by sequencing (Fig. 2A, negative control and sequencing data not shown). In addition, immunohistochemistry in human compact bone sections was performed to corroborate the expression of VIP at protein level in osteocytes (Fig. 2B, arrows). Results revealed VIP presence in osteocytic cells at both mRNA and protein levels.

To determine the expression pattern of the VIP receptors, VPAC1 and VPAC2, their transcript levels were analysed in human osteocytes after 14 days of *in vitro* differentiation by real-time qPCR. Both VPAC1 and VPAC2 transcripts were detected (Fig. 2C), and the presence of the corresponding proteins was further confirmed by Western blot analysis (Fig. 2D), supporting the expression of both receptors in differentiated human osteocytes.

#### Regulation of osteocyte marker gene expression and cell morphology by VIP during *in vitro* differentiation

We next elucidated whether the presence of VIP modulates *in vitro* osteocyte differentiation. After 14 days of osteocyte differentiation in monocultures, in presence or absence of 10<sup>-8</sup>M VIP osteocyte specific gene expression was analysed by real-time qPCR. Exposure to VIP resulted in a significant decrease in gene expression of the mature osteoblast marker *BGLAP* (p-value = 0.0006) (Fig. 3A). At the same time, a significant increase was observed on *MEPE* (p-value=0.0460) and *SOST* (p-value=0.0307), both gene markers associated with late stages of osteocyte differentiation (Fig. 3B, C).

To investigate whether VIP influences the cytoskeletal reorganization required for the morphological transition to the characteristic dendritic morphology of osteocytes, immunofluorescence staining of F-actin was performed after 14 days of *in vitro* induction. Qualitative assessment of the immunofluorescence images (Fig. 3D, supplementary figure 2) demonstrated successful osteocyte differentiation in both control and VIP-treated groups, with development of the typical dendritic outgrowths.

#### VIP modulates RANKL/OPG ratio in differentiating osteocytes

In order to explore the potential modulatory effects of VIP on bone remodelling by regulating osteocyte-mediated coordination of osteoblasts and osteoclasts, we investigated whether this neuropeptide could modulate the RANKL/OPG system in osteocytes. Gene expression of RANKL (*TNFSF11*) and OPG (*TNFRSF11B*) was analysed after 14 days of *in vitro* osteocytogenesis in the presence or absence of VIP by real-time qPCR. Although RANKL transcript levels remain unchanged (Fig. 4A), the presence of VIP significantly increased OPG gene expression (p-value<0.001) in differentiated osteocytes (Fig. 4B), resulting in a significant decrease in the RANKL/OPG ratio (p-value=0.0040) (Fig. 4C).

#### Regulation of bone cell differentiation markers by VIP in triple co-cultures

Next, we explored the role of VIP in a system that mimicked the physiological conditions of bone remodelling. For this propose, triple cultures containing mature osteoblasts, as well as osteocytes and osteoclasts undergoing simultaneous differentiation, were performed in the presence or absence of the neuropeptide. After 14 days in triple culture, gene expression of the involved cell types was examined.

Osteocytes differentiated in the presence of VIP in triple culture exhibited a significant reduction of *BGLAP* mRNA expression (p-value=0.0082) (Fig. 5A), a marker of mature osteoblasts. Furthermore, neuropeptide exposure significantly upregulated *MEPE* gene expression (p-value=0.0043) (Fig. 5B), accompanied by a significant reduction in *SOST* (p-value=0.0015) (Fig. 5C). Regarding osteoblast gene expression,

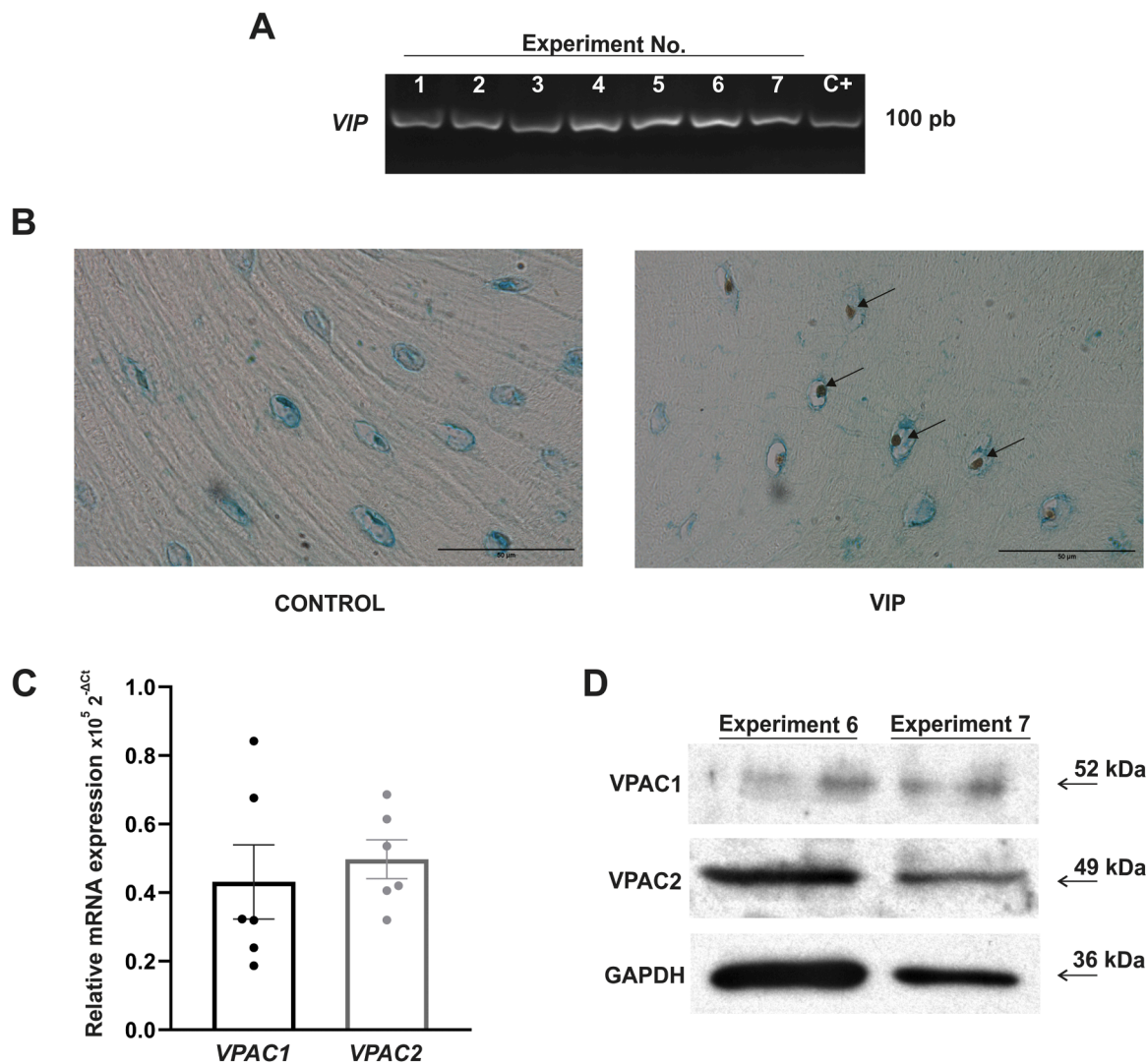


**Fig. 2. Characterizing the VIP/receptor axis in human osteocytes.** A. VIP mRNA expression in human osteocytes of seven different donors differentiated during 14 days in 3D type I collagen gels. Electrophoretic analysis of reverse transcription polymerase chain reaction (RT-PCR) products. mRNA from human osteoblasts was used as positive control (C+). B. Immuno-peroxidase staining of VIP (arrows) in 3  $\mu$ m human compact bone sections (alcian blue and light green counterstained). Images were captured with Olympus BX51 microscope (100x). C. *VPAC1* and *VPAC2* gene expression in *in vitro*-differentiated human osteocytes determined by real time-PCR. Results of six independent experiments are expressed as relative mRNA expression (relative to *ACTB* levels). D. Protein detection of VIP receptors after 14 days of human osteocytes differentiation was determined by western blot and GAPDH was used as a loading control. Representative result is shown.

VIP treatment in triple culture induced a significant downregulation of both *BGLAP* (p-value=0.0159) and *ALPL* (p-value=0.0079) gene expression (Fig. 5D, E).

Finally, when osteoclast-associated genes were characterised, results showed a significant decrease in the expression of master regulator of osteoclastogenesis *NFATC1* (p-value=0.0043), as well as a tendency for decreased *DCSTAMP* expression (p-value=0.2544) when triple cultures were exposed to VIP (Fig. 6A, B). Similarly, a decrease in the expression of *ACP5*, encoding *TRAP* (p-value=0.0722), and *CTSK*, encoding cathepsin k, (p-value=0.0008), two markers associated with resorptive activity, was observed under VIP stimulation (Fig. 6C, D).

#### VIP modulates *RANKL* and *OPG* gene expression in osteoblasts and osteocytes within triple co-cultures

Given that osteogenic lineage cells, including osteoblasts and osteocytes, are considered the main sources of *OPG* and *RANKL*, respectively, playing a fundamental role in regulating bone homeostasis, we examined whether their gene expression (*TNFRSF11B* and *TNFSF11*) was altered in bone triple co-cultures exposed to VIP. In osteoblasts, the

presence of VIP led to a significant decrease in *RANKL* gene expression (p-value = 0.0476) accompanied by an increase in *OPG* mRNA levels (p-value = 0.0149) (Fig. 7A, B), resulting in a significant reduction of the *RANKL/OPG* ratio for this cell type (p-value = 0.0476) (Fig. 7C).

In contrast, although osteocytes showed significantly decreased *RANKL* mRNA levels, they exhibited a downregulation of *OPG* (p-value = 0.456 and p-value = 0.0350, respectively) (Fig. 7D, E). However, the *RANKL/OPG* ratio in osteocytes, showed a significant reduction in the presence of VIP within the triple co culture similar to osteoblasts (p-value = 0.0183) (Fig. 7F).

#### Impact of VIP on cell morphology of osteoblast, osteocytes and osteoclasts in triple co-cultures

Cytoskeletal reorganization and the consequent morphological transitions are critical for the differentiation and functional activity of all three bone cell types present in the triple co-cultures. To evaluate the impact of VIP on mature osteoblasts as well as on differentiating osteocytes and osteoclasts, immunofluorescence staining of F-actin was performed in all three cell types after 14 days of culture.

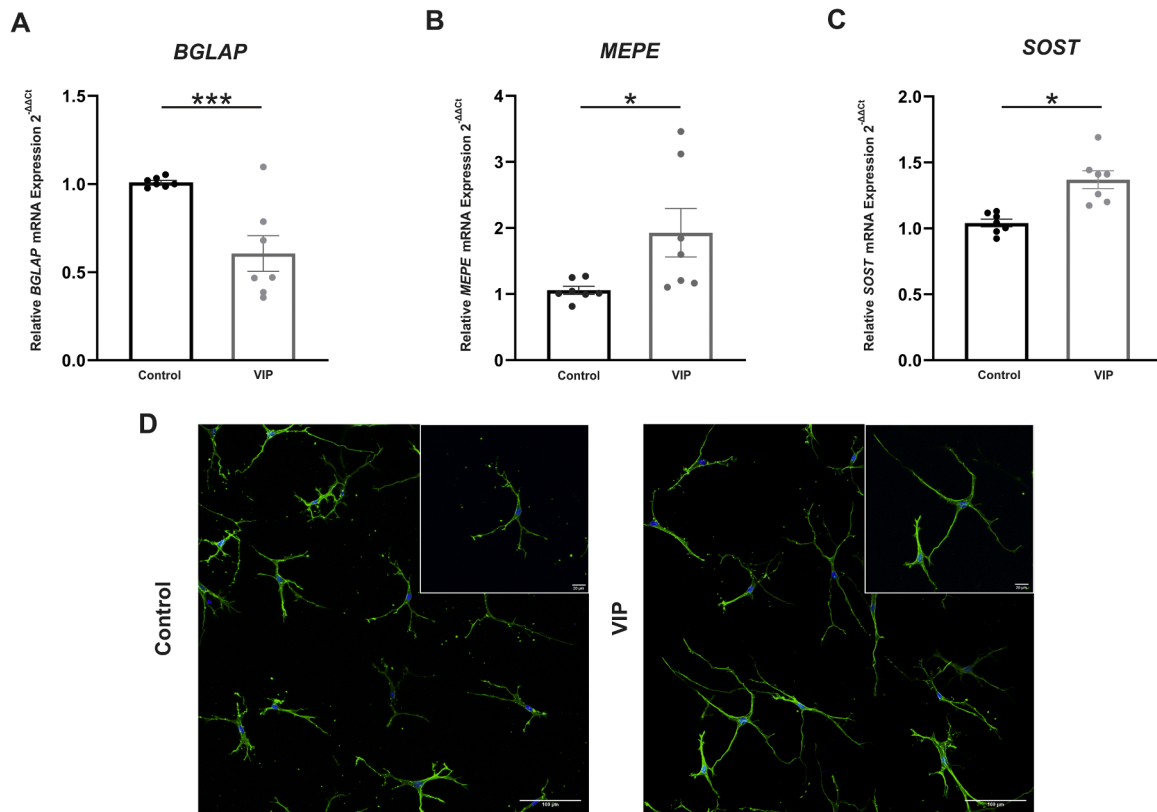


**Fig. 3.** Effect of VIP on osteocyte-associated gene markers expression and morphology during *in vitro* differentiation. *BGLAP* (A), *MEPE* (B), *SOST* (C) mRNA expression levels in differentiated human osteocytes after 14 days of monoculture in 3D type I collagen gels, in absence or presence of VIP  $10^{-8}$  M, determined by real-time PCR. Results are expressed as relative mRNA expression (relative to *ACTB* levels) and referenced to the control group. Seven independent experiments were performed, data points after outlier analysis removal are presented as mean  $\pm$  SEM. T-Test and Mann Whitney U test were performed (\* $p < 0.05$ ; \*\* $p < 0.01$ ; \*\*\* $p < 0.001$ ). **D.** Photomicrographs of the effect of VIP on the actin cytoskeleton in *in vitro*-differentiated osteocytes (Olympus FluoView-1200 confocal microscope, 40x). Detection of F-actin was performed using Phalloidin-iFluor 488 (Abcam, green) and nuclei were counterstained with DAPI (blue). Scale bars represent 200  $\mu$ m (white) and 50  $\mu$ m (yellow). Representative result is shown.

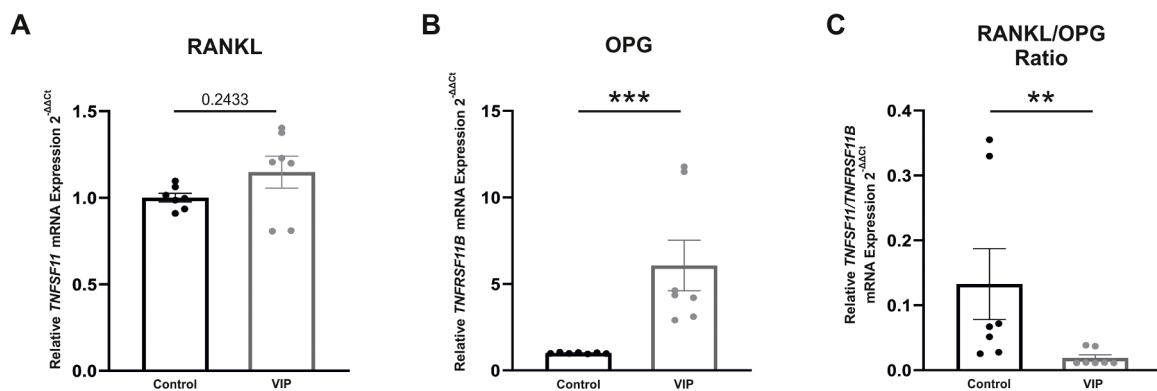


**Fig. 4.** VIP modulates RANKL/OPG ratio in osteocytes. Relative mRNA expression of *TNFSF11* (RANKL) (A) and *TNFRSF11B* (OPG) (B) in human osteocytes after 14 days of *in vitro* differentiation in the absence or presence of VIP  $10^{-8}$  M, determined by real-time PCR. **C.** RANKL/OPG (*TNFSF11/TNFRSF11B*) ratio on gene expression level. Results are expressed as relative mRNA expression (relative to *ACTB* levels) and referenced to the control group. Seven independent experiments were performed, data points after outlier analysis removal are presented as mean  $\pm$  SEM. T-Test and Mann Whitney U test were performed (\*\* $p < 0.01$ ; \*\*\* $p < 0.001$ ).

Similar to osteocyte differentiation experiments in 3D collagen gels, qualitative assessment of the immunofluorescence images confirmed osteocyte differentiation in both control and VIP-treated groups, with development of extended dendritic processes (Fig. 8B). Besides, we recognized a reduction in osteoclast density accompanied by disorganized actin structures that impaired the formation of the sealing actin ring required for resorption lacunae development (Fig. 8A).

Furthermore, no osteoblasts were observed in the lower compartment, supporting the absence of cell type mixing in the triple co-culture model (data not shown). Finally, no changes were reported on osteoblast cell morphology between control and VIP treatment (Fig. 8C).

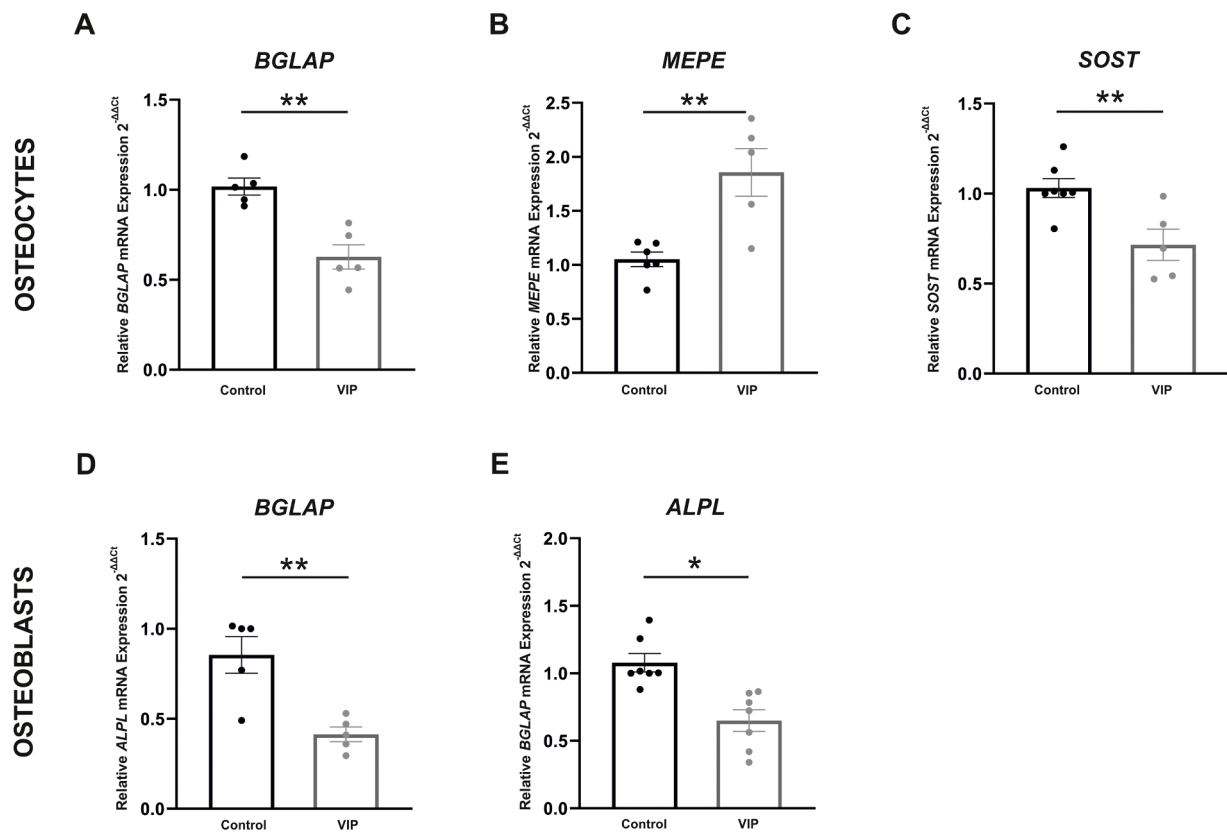


**Fig. 5.** Effect of VIP on osteoblast and osteocyte gene markers in bone triple co-cultures. Relative mRNA expression of *BGLAP* (A, D), *MEPE* (B), *SOST* (C) and *ALPL* (E) in osteoblasts and osteocytes after 14 days of triple co-culture, in absence or presence of VIP  $10^{-8}$  M, was determined by real-time PCR. Results are expressed as relative mRNA expression (relative to *ACTB* levels) and referenced to the control group. Seven independent experiments were performed, data points after outlier analysis removal are presented as mean  $\pm$  SEM. T-Test and Mann Whitney U test were performed (\* $p < 0.05$ ; \*\* $p < 0.01$ ).

## Discussion

Extensive research described the molecular and cellular pathways that mediate the regulatory actions of VIP in bone remodelling. However, its impact on osteocyte biology has not been elucidated yet, probably due to the technical difficulty involved in the *in vitro* differentiation of primary osteocytes. In the present study, by establishing 3D collagen gel cultures for osteocyte differentiation, we report for the first time that human osteocytes not only express VIP but also its specific receptors, suggesting a potential autocrine signalling mechanism. Moreover, our data demonstrate that exogenous VIP enhances the *in vitro* differentiation of human osteocytes, raising the possibility of a direct modulatory role of this neuropeptide in osteocyte biology. Consistently, our findings in a more complex cellular context using a triple co culture model indicate that, in the presence of VIP, the osteoblast to osteocyte transition is enhanced toward an osteoprotective phenotype. This phenotype is characterized by reduced sclerostin levels and a lower RANKL/OPG ratio, promoting osteogenesis while limiting osteoclastogenesis. These results reveal novel insights into VIP mediated cellular crosstalk in bone, highlighting its modulatory influence on the orchestrating activity of osteocytes, which underlies its reported bone homeostatic effects.<sup>16,23,24,26,27</sup>

Our initial objective was to characterize the VIP/receptor axis in human osteocytes and to determine whether these cells, as terminally differentiated osteoblasts, retain the expression of VIP and its specific receptors, previously reported in *in vitro*-differentiated human osteoblasts.<sup>27</sup> As anticipated, VIP transcripts were detected in 3D differentiated human osteocytes and confirmed in bone matrix embedded cells through immunohistochemical analysis of compact bone sections, in agreement with a previous report describing VIP expression in osteocyte

like cells within the subchondral bone of osteoarthritic patients.<sup>31</sup> These findings suggest that osteocytes may act as an additional source of VIP within the bone microenvironment contributing to further increase its local levels, similar to reports on the neuropeptide NPY.<sup>36</sup> Furthermore, the elevated VIP levels previously reported by Kanemitsu et al. in the subchondral bone of osteoarthritic patients<sup>31</sup> suggests that this regulatory mechanism may also function under pathological conditions. Moreover, our results provide the first evidence for VPAC1 and VPAC2 expression in human osteocytes, consistent with the preservation of receptor expression previously demonstrated in *in vitro*-differentiated human osteoblasts<sup>27</sup> and also reported in human periosteum derived osteoblastic cells (SaM 1) and osteosarcoma derived cell lines (SaOS 2, HOS, and MG 63).<sup>37–40</sup> The presence of both receptors suggests that VIP can directly modulate osteocyte activity and, together with its local production by osteogenic lineage cells, supports the concept of VIP acting as an osteocytic autocrine and paracrine factor within the bone microenvironment.

Accumulating evidence has established VIP as an endogenous osteoinductive factor, directly promoting the osteogenic differentiation of human and rat BM-MSCs.<sup>26,27</sup> As osteocytes express the receptors mediating VIP activity, the present study explored its potential role in regulating the transition from mature osteoblasts to osteocytes. Our results demonstrate that in *in vitro* 3D differentiated osteocytes, VIP exposure upregulated the anti mineralization genes *MEPE* and *SOST*, the latter encoding the bone formation inhibitor sclerostin, both well-established markers of mature osteocytes.<sup>41</sup> These data align with findings in a murine model of alveolar bone healing, where VIP increased osteogenic related markers, along with upregulation of osteocytic genes such as *SOST*.<sup>42</sup> Besides, we also observed a significant reduction in the mature osteoblast marker *BGLAP* in osteocytes

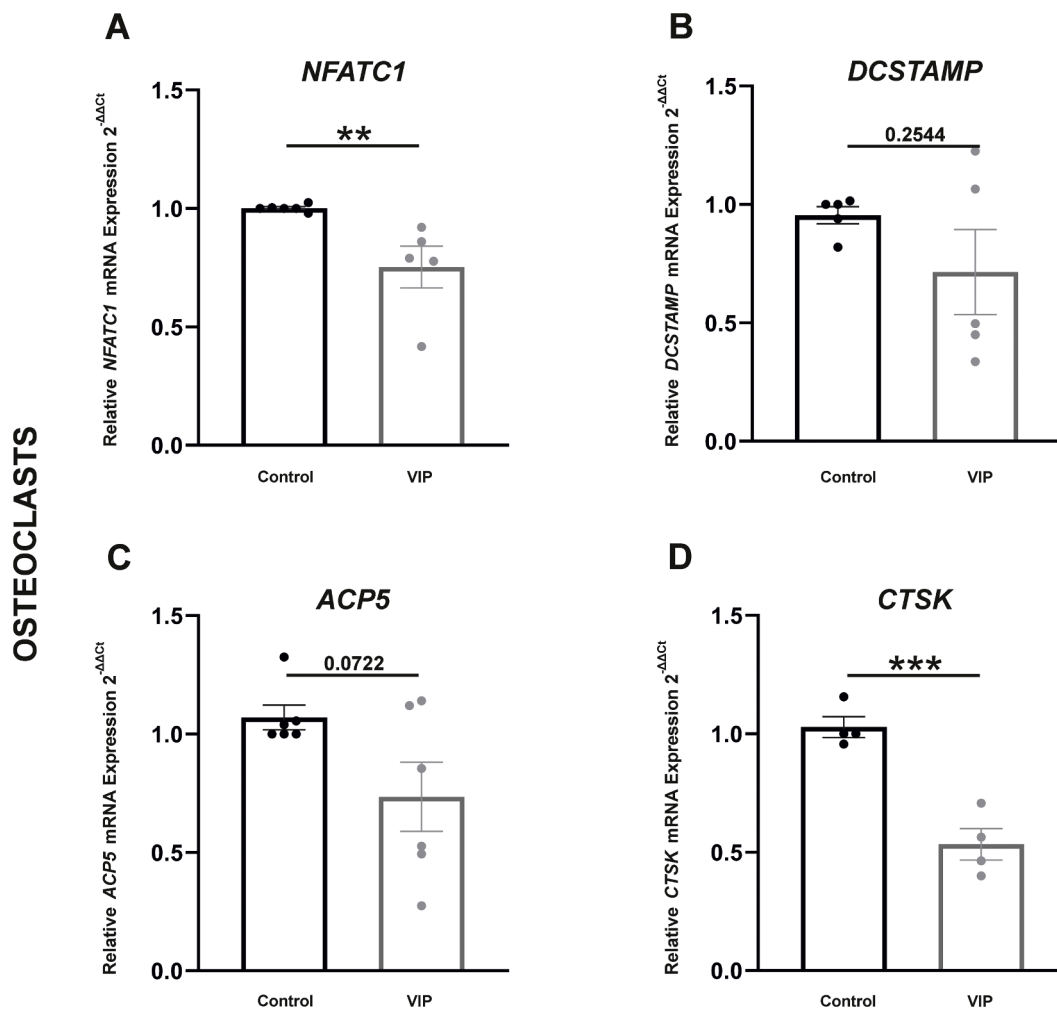


**Fig. 6.** VIP down-regulates the expression of osteoclast-specific markers in triple co-cultures. (A) *NFATC1*, (B) *DCSTAMP*, (C) *ACP5* and (D) *CTSK* mRNA expression levels in differentiated osteoclasts after 14 days of triple co-culture, in absence or presence of VIP  $10^{-8}$  M, determined by real-time PCR. Results are expressed as relative mRNA expression (relative to *ACTB* levels) and referenced to the control group. Seven independent experiments were performed, data points after outlier analysis removal are presented as mean  $\pm$  SEM. T-Test and Mann Whitney U test were performed (\*\* $p < 0.01$ ; \*\*\* $p < 0.001$ ).

differentiated under VIP stimulation, consistent with an enhancement of the osteocytogenic process, during which osteoblasts progressively downregulate bone matrix production.<sup>43</sup> Additionally, as osteocytogenesis requires cytoskeletal plasticity for the formation of dendritic extensions within the canalicular network,<sup>1</sup> and given that VIP has been shown to induce F actin reorganization in osteogenic cells,<sup>27</sup> we examined the cytoskeletal architecture of osteocytes exposed to VIP. Qualitative morphological analysis indicated that VIP-stimulated osteocytes retained their characteristic stellate morphology and exhibited extended dendritic projections, potentially reflecting progression in the differentiation process.<sup>43</sup> Therefore, the present findings support the hypothesis that VIP may facilitate the transition from osteoblast to osteocyte, inducing osteocyte-specific gene expression, and enabling cytoskeletal rearrangements required for extensive dendritic branching.

As central regulators of bone homeostasis, osteocytes exert paracrine effects on osteoblasts and osteoclasts through direct cell-cell interactions and the release of regulatory molecules like RANKL and OPG.<sup>43,44</sup> As both cytokines have been identified as targets of VIP in its osteoblast-mediated anti-osteoclastogenic effects,<sup>27,45</sup> and given that the osteoprotective activity of this neuropeptide in both animal models and early arthritis patients has been linked to a reduced RANKL/OPG ratio,<sup>16,24</sup> we aimed to determine whether a similar regulatory effect occurs in osteocytes. Our data reveal a significant increase in the OPG mRNA levels in osteocytes differentiated in the presence of VIP,

consistent with its reported ability to counteract the inhibitory effect of  $1,25(\text{OH})_2$ -vitamin  $\text{D}_3$  on OPG expression in mouse bone marrow cultures<sup>45</sup> and to upregulate OPG in MC3T3-E1 pre-osteoblastic cells.<sup>46</sup> Consequently, we also detected a decrease in the osteocytic RANKL/OPG ratio, similar to that observed in *in vitro*-differentiated human osteoblasts,<sup>27</sup> supporting the notion that VIP may also exert anti-osteoclastogenic effects through the regulation of these osteocyte-derived factors.

However, to fully assess the modulatory effects of VIP on osteocyte-mediated bone homeostasis, it is essential to consider the reciprocal interactions among osteoblasts, osteoclasts and osteocytes. Therefore, to better mimic the bone remodelling process, we analysed the impact of the neuropeptide in the triple co-culture system, in which osteocytes and osteoclasts were simultaneously differentiated from their progenitors in the presence of mature osteoblasts.<sup>34</sup> In line with our findings in osteocyte monocultures, exposure to VIP downregulated the mature osteoblast marker *BGLAP* in differentiating osteocytes, while concurrently increasing the osteocytic marker *MEPE*, and inducing a more pronounced dendritic morphology, characteristic of fully differentiated osteocytes. In contrast, our results demonstrated that VIP significantly downregulated *SOST* expression in triple culture, a finding that should be interpreted within the specific context of the triple co-culture, as sclerostin not only acts as a direct inhibitor of osteoblast differentiation<sup>6,47–49</sup> but also indirectly promotes osteoclastogenesis through

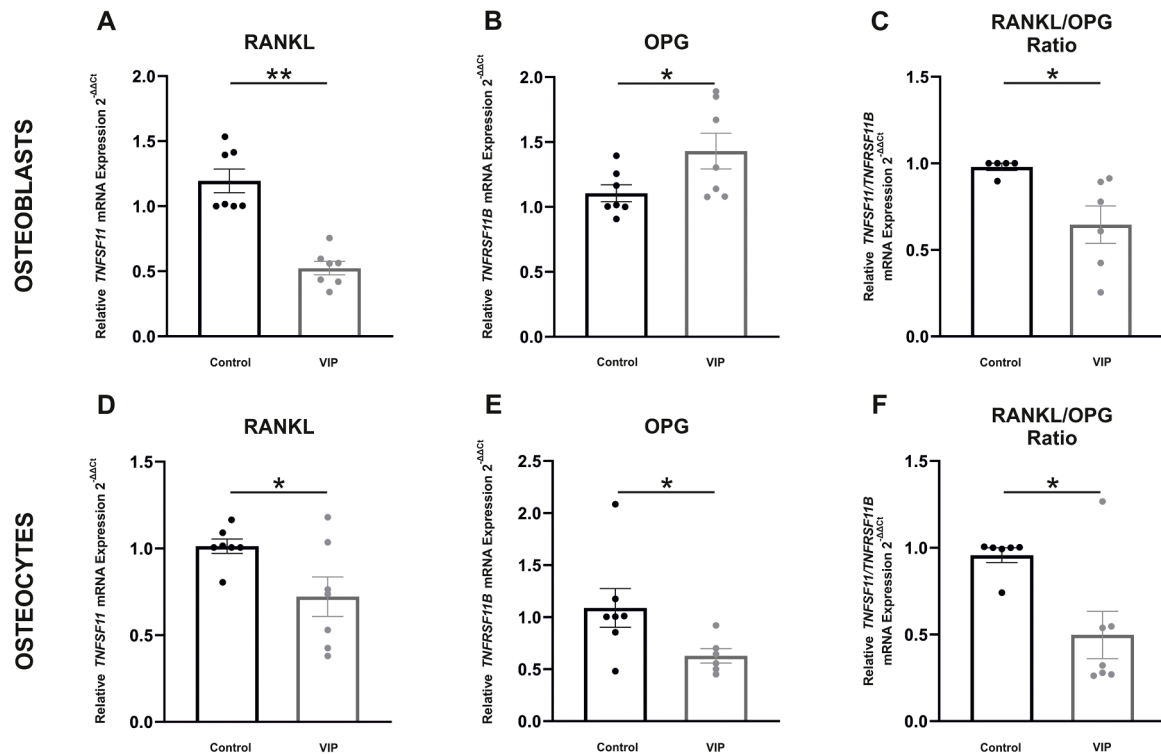


**Fig. 7.** Effect of VIP on osteoblast and osteocyte *RANKL* and *OPG* gene expression in triple co-cultures. Relative mRNA expression of *TNFSF11* (*RANKL*) (A, D) and *TNFRSF11B* (*OPG*) (B, E) after 14 days of triple co-culture in absence or presence of VIP  $10^{-8}$  M was determined by real-time PCR in osteoblasts and osteocytes. *RANKL/OPG* (*TNFSF11/TNFRSF11B*) (C, F) ratio of gene expression values. Results are expressed as relative mRNA expression (relative to *ACTB* levels) and referenced to the control group. Seven independent experiments were performed, data points after outlier analysis removal are presented as mean  $\pm$  SEM. *T*-Test and Mann Whitney U test were performed (\* $p < 0.05$ ; \*\* $p < 0.01$ ).

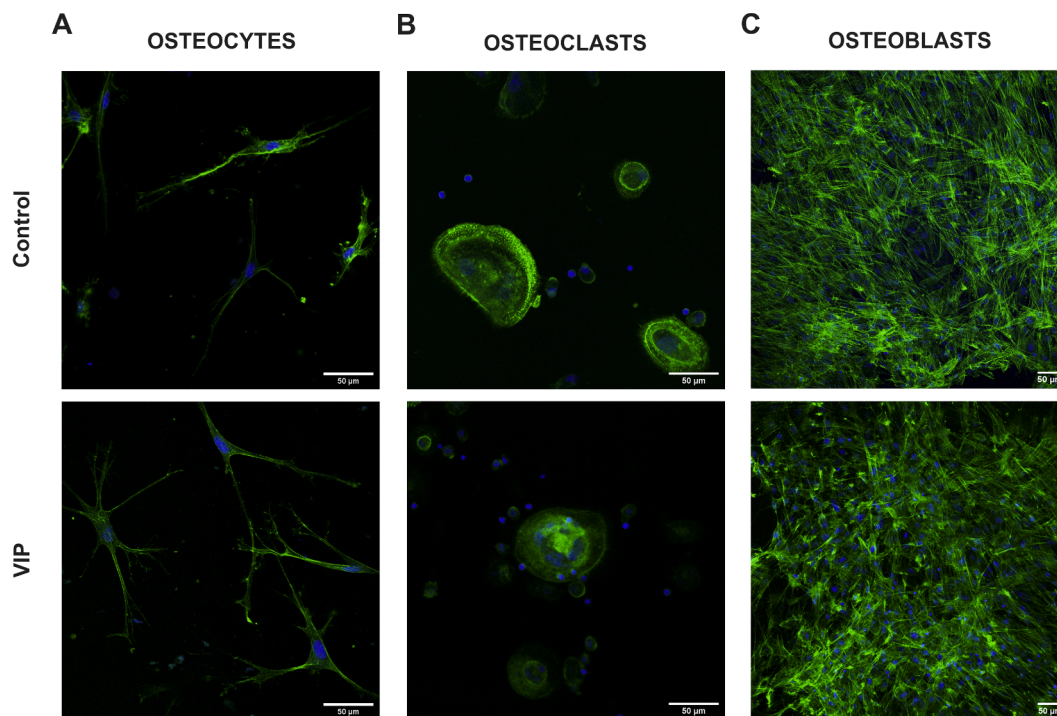


**Fig. 8.** Cell morphology of osteoclasts, osteocytes and osteoblasts in triple co-culture in the absence or presence of VIP. Photomicrographs of the effect of VIP presence on the actin cytoskeleton in osteocytes (A), osteoclasts(B) and osteoblasts (C) after 14 days of triple co-cultures (Olympus FluoView-1200 confocal microscope, 40x). Detection of F-actin was performed using Phalloidin-iFluor 488 (Abcam, green) and nuclei were counterstained with DAPI (blue).

osteoblast-mediated signalling.<sup>50,51</sup> Thus, by downregulating osteocytic sclerostin, VIP may promote the differentiation of osteogenic lineage

cells and further facilitate osteocytogenesis, consistent with the well established inhibitory role of this protein in the mature osteoblast to osteocyte transition.<sup>52</sup> This hypothesis aligns with the significant decrease in *BGLAP* and *ALPL* expression detected in mature osteoblasts cultivated in triple cultures exposed to VIP, reflecting a reduction in the mineralizing activity required for their transition into osteocytes.<sup>53</sup>

In this context, the downregulation of *SOST* observed in VIP treated bone triple co-cultures may be related to the reduced osteoblastic RANKL/OPG ratio, consistent with the role of sclerostin in enhancing RANKL while suppressing OPG in mature osteoblasts.<sup>50</sup> In this sense, our findings from the triple co culture model demonstrate a marked reduction in osteoclast differentiation markers (*NFATC1* and *DCSTAMP*) and resorptive activity markers (*ACP5* and *CTSK*) in the presence of VIP, accompanied by disruption of the actin cytoskeletal reorganization essential for osteoclast resorptive function. This decrease in osteoclastogenic gene and morphological markers likely reflects both the well-established direct inhibitory effect of VIP on osteoclasts biology<sup>16,20,45</sup> and the downstream consequences of the reduced RANKL/OPG ratio observed in osteoblasts.

Although multiple cell types contribute to RANKL production during bone remodelling, osteocytes are widely recognized as the predominant source of functional RANKL driving osteoclastogenesis.<sup>43</sup> Interestingly, within the bone triple co-culture model, VIP stimulation led to a marked decrease in osteocyte RANKL expression, an effect that was not observed under monoculture conditions. This microenvironment-dependent response could partly result from the VIP induced decrease in sclerostin, which promotes a pro osteoclastogenic phenotype in human primary pre osteocytes and in the murine osteocyte like cell line MLO Y4 by stimulating RANKL expression.<sup>50,51,54</sup> Thus, the reduction of osteocytic *SOST* observed in the presence of VIP could not only attenuate the osteocyte mediated inhibition of osteogenesis but also represent an additional mechanism underlying the anti osteoclastogenic effects of VIP, potentially interfering with the RANKL dependent pathway by which osteocytes support osteoclast differentiation. Conversely, our data also reveal that the OPG gene expression is downregulated in osteocytes exposed to VIP within the triple co-culture. This could potentially compromise its anti-osteoclastogenic action, as OPG functions as a soluble decoy receptor for RANKL, thereby preventing osteoclast formation and bone resorption. Nevertheless, this effect is not expected to substantially impact bone cellular crosstalk, since it does not alter the OPG dominance in the osteocytic RANKL/OPG ratio. Furthermore, osteoblasts are widely recognized as the predominant source of OPG within the bone microenvironment.<sup>55,56</sup> Despite this, osteocytic OPG may play an important role in the mechanisms that regulate subcellular RANKL trafficking.<sup>57,58</sup> Given that membrane-bound RANKL but not soluble RANKL constitutes the physiologically active form required for osteoclast formation,<sup>9,10</sup> the VIP-induced decrease in osteocytic OPG expression could impair RANKL trafficking to the cell surface, thereby further reinforcing an anti-osteoclastogenic profile.

In summary, our findings indicate that VIP may function as an autocrine and paracrine modulator of osteoblast and osteocyte activity, introducing a new regulatory component within the neuro-osteogenic pathway. In addition, our results show that VIP promotes osteocytogenesis, leading to the acquisition of an osteoprotective phenotype characterized by reduced sclerostin expression. This decrease not only attenuates osteocyte mediated inhibitory signalling toward osteoblasts but also contributes to an anti osteoclastogenic profile by lowering the osteoblastic RANKL/OPG ratio. This suppressive effect of VIP on osteoclast biology may be further reinforced by downregulation of RANKL in osteocytes, resulting in a reduced osteocytic RANKL/OPG ratio, along with a concomitant decrease in OPG expression that could impair RANKL localization to the osteocyte membrane.

Although additional studies are needed to better understand the mechanisms involved, our findings represent an important advancement in understanding the role of VIP in osteocyte-mediated regulation of bone metabolism. This research represents a significant step toward

exploring new therapeutic targets for a wide range of musculoskeletal disorders characterized by impaired bone homeostasis.

## Statements and declarations

### Funding

This research was funded by grants RD24/0007/0014 and RD21/0002/0004 from the Ministerio de Economía y Competitividad (Instituto de Salud Carlos III), co-funded by European regional development fund (ERDF) and by the UCM grants PR12/24-31568 and PR12/24-31572. DC-V was awarded with an EMBO Scientific Exchange Grant (SEG 10287). KW was awarded a scholarship funded by and in cooperation with the Saxon Ministry for Higher Education and Arts and the Studentenwerk Dresden.

### Data availability

Data and further details regarding the manuscript will be made available by request to the corresponding author.

### Ethics approval

This study was performed in line with the principles of the Declaration of Helsinki. Approval was granted by the Ethics Committee of the San Carlos Clinical Hospital (25/112-E, Feb 2025). Primary human pre-osteoblasts were isolated from human femoral heads after informed consent (approval by the ethics commission of TU Dresden, EK 303082014).

### CRediT authorship contribution statement

**David Castro-Vázquez:** Writing – original draft, Methodology, Investigation, Formal analysis, Data curation, Conceptualization. **Iván García-López:** Writing – original draft, Methodology, Investigation, Formal analysis, Data curation. **Katharina Wirsig:** Writing – review & editing, Methodology, Investigation. **Paula Arribas-Castaño:** Writing – original draft, Formal analysis, Data curation. **Rosa P. Gomariz:** Writing – review & editing, Conceptualization. **Carmen Martínez:** Writing – review & editing, Project administration. **Yasmina Juarranz:** Writing – review & editing, Supervision, Project administration. **Anne Bernhardt:** Writing – review & editing, Supervision, Methodology, Investigation, Conceptualization. **Mar Carrión:** Writing – review & editing, Writing – original draft, Supervision, Investigation, Formal analysis, Data curation, Conceptualization.

### Conflict of interest

All authors have read the journal's policy on disclosure of potential conflicts of interest. The authors declare no competing interests.

### Acknowledgements

We thank the Genomics and Fluorescence Microscopy Centres of Complutense University for the use of their facilities. We are grateful to all donors and the collaborating clinicians for their participation in this study. We also appreciate the assistance of Isabel Montero, for her assistance with histology techniques.

### Supplementary materials

Supplementary material associated with this article can be found, in the online version, at [doi:10.1016/j.trsl.2026.04.004](https://doi.org/10.1016/j.trsl.2026.04.004).

## References

- Bolamperti S, Villa I, Rubinacci A. Bone remodeling: an operational process ensuring survival and bone mechanical competence. *Bone Res.* 2022;10:48. <https://doi.org/10.1038/s41413-022-00219-8>.
- Krasnova O, Neganova I. Assembling the puzzle pieces. Insights for in vitro bone remodeling. *Stem Cell Rev Rep.* 2023;19:1635–1658. <https://doi.org/10.1007/s12015-023-10558-6>.
- Sun W, Ye B, Chen S, Zeng L, Lu H, Wan Y, et al. Neuro-bone tissue engineering: emerging mechanisms, potential strategies, and current challenges. *Bone Res.* 2023; 11:65. <https://doi.org/10.1038/s41413-023-00302-8>.
- Liu S, Chen T, Wang R, Huang H, Fu S, Zhao Y, et al. Exploring the effect of the "quaternary regulation" theory of "peripheral nerve-angiogenesis-osteoclast-osteogenesis" on osteoporosis based on neuropeptides. *Front Endocrinol.* 2022;13, 908043. <https://doi.org/10.3389/fendo.2022.908043>.
- Choi JUA, Kijas AW, Lauko J, Rowan AE. The mechanosensory role of osteocytes and implications for bone health and disease states. *Front Cell Dev Biol.* 2021;9, 770143. <https://doi.org/10.3389/fcell.2021.770143>.
- Robling AG, Bonewald LF. The osteocyte: new insights. *Annu Rev Physiol.* 2020;82: 485–506. <https://doi.org/10.1146/annurev-physiol-021119-034332>.
- Florencio-Silva R, Sasso GR, Sasso-Cerri E, Simoes MJ, Cerri PS. Biology of bone tissue: structure, function, and factors that influence bone cells. *Biomed Res Int.* 2015;2015, 421746. <https://doi.org/10.1155/2015/421746>.
- Dallas SL, Prideaux M, Bonewald LF. The osteocyte: an endocrine cell and more. *Endocr Rev.* 2013;34:658–690. <https://doi.org/10.1210/er.2012-1026>.
- Nakashima T, Hayashi M, Fukunaga T, Kurata K, Oh-Hora M, Feng JQ, et al. Evidence for osteocyte regulation of bone homeostasis through RANKL expression. *Nat Med.* 2011;17:1231–1234. <https://doi.org/10.1038/nm.2452>.
- Xiong J, Onal M, Jilka RL, Weinstein RS, Manolagas SC, O'Brien CA. Matrix-embedded cells control osteoclast formation. *Nat Med.* 2011;17:1235–1241. <https://doi.org/10.1038/nm.2448>.
- Takegahara N, Kim H, Choi Y. RANKL biology. *Bone.* 2022;159, 116353. <https://doi.org/10.1016/j.bone.2022.116353>.
- Park JH, Lee NK, Lee SY. Current understanding of RANK signaling in osteoclast differentiation and maturation. *Mol Cells.* 2017;40:706–713. <https://doi.org/10.14348/molcells.2017.0225>.
- Takayanagi H, Kim S, Koga T, Nishina H, Isshiki M, Yoshida H, et al. Induction and activation of the transcription factor NFATc1 (NFAT2) integrate RANKL signaling in terminal differentiation of osteoclasts. *Dev Cell.* 2002;3:889–901. [https://doi.org/10.1016/s1534-5807\(02\)00369-6](https://doi.org/10.1016/s1534-5807(02)00369-6).
- Udagawa N, Koide M, Nakamura M, Nakamichi Y, Yamashita T, Uehara S, et al. Osteoclast differentiation by RANKL and OPG signaling pathways. *J Bone Min Metab.* 2021;39:19–26. <https://doi.org/10.1007/s00774-020-01162-6>.
- Lerner UH, Persson E. Osteotropic effects by the neuropeptides calcitonin gene-related peptide, substance P and vasoactive intestinal peptide. *J Musculoskelet Neuronal Interact.* 2008;8:154–165.
- Castro-Vázquez D, Lamana A, Arribas-Castaño P, Gutierrez-Canas I, Villanueva-Romero R, Perez-García S, et al. (2021) The neuropeptide VIP limits Human osteoclastogenesis: clinical associations with bone metabolism markers in patients with early arthritis. *Biomedicine* 9. <https://doi.org/10.3390/biomedicine9121880>.
- Qu H, Zhuang Y, Zhu L, Zhao Z, Wang K. The effects of vasoactive intestinal peptide on RANKL-induced osteoclast formation. *Ann Transl Med.* 2021;9(2):127. <https://doi.org/10.21037/atm-20-7607>.
- Eger M, Liron T, Hiram-Bab S, Awida Z, Giladi E, Dangoor D, et al. Therapeutic potential of vasoactive intestinal peptide and its derivative stearyl-norleucine-VIP in inflammation-induced osteolysis. *Front Pharmacol.* 2021;12, 638128. <https://doi.org/10.3389/fphar.2021.638128>.
- Muschter D, Schaefer N, Stangl H, Straub RH, Graessel S. Sympathetic neurotransmitters modulate osteoclastogenesis and osteoclast activity in the context of collagen-induced arthritis. *Plos One.* 2015;10, e0139726. <https://doi.org/10.1371/journal.pone.0139726>.
- Lundberg P, Lie A, Bjurholm A, Lehenkari PP, Horton MA, Lerner UH, et al. Vasoactive intestinal peptide regulates osteoclast activity via specific binding sites on both osteoclasts and osteoblasts. *Bone.* 2000;27:803–810. [https://doi.org/10.1016/s8756-3282\(00\)00394-x](https://doi.org/10.1016/s8756-3282(00)00394-x).
- Lerner UH. Neuropeptidergic regulation of bone resorption and bone formation. *J Musculoskelet Neuronal Interact.* 2002;2:440–447.
- Deng S, Xi Y, Wang H, Hao J, Niu X, Li W, et al. Regulatory effect of vasoactive intestinal peptide on the balance of Treg and Th17 in collagen-induced arthritis. *Cell Immunol.* 2010;265:105–110. <https://doi.org/10.1016/j.cellimm.2010.07.010>.
- Delgado M, Abad C, Martínez C, Laceta J, Gomariz RP. Vasoactive intestinal peptide prevents experimental arthritis by downregulating both autoimmune and inflammatory components of the disease. *Nat Med.* 2001;7:563–568. <https://doi.org/10.1038/87887>.
- Juarranz Y, Abad C, Martínez C, Arranz A, Gutierrez-Canas I, Rosignoli F, et al. Protective effect of vasoactive intestinal peptide on bone destruction in the collagen-induced arthritis model of rheumatoid arthritis. *Arthritis Res Ther.* 2005;7: R1034–R1045. <https://doi.org/10.1186/ar1779>.
- Gurkan A, Emingil G, Nizam N, Doganavsargil B, Sezak M, Kutukculer N, et al. Therapeutic efficacy of vasoactive intestinal peptide in escherichia coli lipopolysaccharide-induced experimental periodontitis in rats. *J Periodontol.* 2009; 80:1655–1664. <https://doi.org/10.1902/jop.2009.090031>.
- Shi L, Feng L, Zhu ML, Yang ZM, Wu TY, Xu J, et al. Vasoactive intestinal peptide stimulates bone marrow-mesenchymal stem cells osteogenesis differentiation by activating wnt/beta-catenin signaling pathway and promotes rat skull defect repair. *Stem Cells Dev.* 2020;29:655–666. <https://doi.org/10.1089/scd.2019.0148>.
- Castro-Vázquez D, Arribas-Castaño P, García-López I, Gutiérrez-Canas I, Perez-García S, Lamana A, et al. Vasoactive intestinal peptide exerts an osteoinductive effect in human mesenchymal stem cells. *Biofactors.* 2024;50(6):1148–1160. <https://doi.org/10.1002/biof.2062>.
- Shi L, Liu Y, Yang Z, Wu T, Lo HT, Xu J, et al. Vasoactive intestinal peptide promotes fracture healing in sympathetomized mice. *Calcif Tissue Int.* 2021;109:55–65. <https://doi.org/10.1007/s00223-021-00820-9>.
- Hohmann EL, Elde RP, Rysavy JA, Einzig S, Gebhard RL. Innervation of periosteum and bone by sympathetic vasoactive intestinal peptide-containing nerve fibers. *Science.* 1986;232:868–871. <https://doi.org/10.1126/science.3518059>.
- Xiao J, Yu WF, Wang XR, Wang B, Chen JW, Liu Y, et al. Correlation between neuropeptide distribution, cancellous bone microstructure and joint pain in postmenopausal women with osteoarthritis and osteoporosis. *Neuropeptides.* 2016; 57:79–85. <https://doi.org/10.1016/j.npep.2015.12.006>.
- Kanemitsu M, Nakasa T, Shirakawa Y, Ishikawa M, Miyaki S, Adachi N. Role of vasoactive intestinal peptide in the progression of osteoarthritis through bone sclerosis and angiogenesis in subchondral bone. *J Orthop Sci.* 2020;25:897–906. <https://doi.org/10.1016/j.jos.2019.11.010>.
- Martinez C, Juarranz Y, Gutierrez-Canas I, Carrion M, Perez-García S, Villanueva-Romero R, et al. A clinical approach for the use of VIP axis in inflammatory and autoimmune diseases. *Int J Mol Sci.* 2019;21(1):100. <https://doi.org/10.3390/ijms21010065>.
- Bernhardt A, Wolf S, Weiser E, Vater C, Gelinsky M. An improved method to isolate primary human osteocytes from bone. *Biomed Tech.* 2020;65:107–111. <https://doi.org/10.1515/bmt-2018-0185>.
- Wirsig K, Bacova J, Richter RF, Hintze V, Bernhardt A. Cellular response of advanced triple cultures of human osteocytes, osteoblasts and osteoclasts to high sulfated hyaluronan (sHA3). *Mater Today Bio.* 2024;25, 101006. <https://doi.org/10.1016/j.mtbio.2024.101006>.
- Bernhardt A, Skottke J, von Witzleben M, Gelinsky M. Triple culture of primary human osteoblasts, osteoclasts and osteocytes as an in vitro bone model. *Int J Mol Sci.* 2021;22(14), 7316. <https://doi.org/10.3390/ijms22147316>.
- Wu JQ, Jiang N, Yu B. Mechanisms of action of neuropeptide Y on stem cells and its potential applications in orthopaedic disorders. *World J Stem Cells.* 2020;12: 986–1000. <https://doi.org/10.4252/wjsc.v12.i9.986>.
- Hohmann EL, Tashjian Jr AH. Functional receptors for vasoactive intestinal peptide on human osteosarcoma cells. *Endocrinology.* 1984;114:1321–1327. <https://doi.org/10.1210/endo-114-4-1321>.
- Bjurholm A, Kreicbergs A, Schultzberg M, Lerner UH. Neuroendocrine regulation of cyclic AMP formation in osteoblastic cell lines (UMR-106-01, ROS 17/2.8, MC3T3-E1, and Saos-2) and primary bone cells. *J Bone Min Res.* 1992;7:1011–1019. <https://doi.org/10.1002/jbmr.5650070903>.
- Togari A, Arai M, Mizutani S, Mizutani S, Koshihara Y, Nagatsu T. Expression of mRNAs for neuropeptide receptors and beta-adrenergic receptors in human osteoblasts and human osteogenic sarcoma cells. *Neurosci Lett.* 1997;233:125–128. [https://doi.org/10.1016/s0304-3940\(97\)00649-6](https://doi.org/10.1016/s0304-3940(97)00649-6).
- Lundberg P, Lundgren I, Mukohyama H, Lehenkari PP, Horton MA, Lerner UH. Vasoactive intestinal peptide (VIP)/pituitary adenylate cyclase-activating peptide receptor subtypes in mouse calvarial osteoblasts: presence of VIP-2 receptors and differentiation-induced expression of VIP-1 receptors. *Endocrinology.* 2001;142: 339–347. <https://doi.org/10.1210/endo.142.1.7912>.
- Kitase Y, Prideaux M. Targeting osteocytes vs osteoblasts. *Bone.* 2023;170, 116724. <https://doi.org/10.1016/j.bone.2023.116724>.
- Azevedo MCS, Fonseca AC, Colavite PM, Melchades JL, Tabanez AP, Codo AC, et al. Macrophage polarization and alveolar bone healing outcome: despite a significant M2 polarizing effect, VIP and PACAP treatments present a minor impact in alveolar bone healing in homeostatic conditions. *Front Immunol.* 2021;12, 782566. <https://doi.org/10.3389/fimmu.2021.782566>.
- Marahleh A, Kitauro H, Ohori F, Noguchi T, Mizoguchi I. The osteocyte and its osteoclastogenic potential. *Front Endocrinol.* 2023;14, 1121727. <https://doi.org/10.3389/fendo.2023.1121727>.
- Delgado-Calle J, Bellido T. The osteocyte as a signaling cell. *Physiol Rev.* 2022;102: 379–410. <https://doi.org/10.1152/physrev.00043.2020>.
- Mukohyama H, Ransjo M, Taniguchi H, Ohyama T, Lerner UH. The inhibitory effects of vasoactive intestinal peptide and pituitary adenylate cyclase-activating polypeptide on osteoclast formation are associated with upregulation of osteoprotegerin and downregulation of RANKL and RANK. *Biochem Biophys Res Commun.* 2000;271:158–163. <https://doi.org/10.1006/bbrc.2000.2599>.
- Yoo YM, Kwag JH, Kim KH, Kim CH. Effects of neuropeptides and mechanical loading on bone cell resorption in vitro. *Int J Mol Sci.* 2014;15:5874–5883. <https://doi.org/10.3390/ijms15045874>.
- Semenov M, Tamai K, Xi H. SOST is a ligand for LRP5/LRP6 and a wnt signaling inhibitor. *J Biol Chem.* 2005;280:26770–26775. <https://doi.org/10.1074/jbc.M504308200>.
- Tresguerres FGF, Torres J, Lopez-Quiles J, Hernandez G, Vega JA, Tresguerres IF. The osteocyte: a multifunctional cell within the bone. *Ann Anat.* 2020;227, 151422. <https://doi.org/10.1016/j.aanat.2019.151422>.
- van Bezooijen RL, Roelen BAJ, Visser A, van der Wee-Pals L, de Wilt E, Karperien M, et al. Sclerostin is an osteocyte-expressed negative regulator of bone formation, but not a classical BMP antagonist. *J Exp Med.* 2004;199:805–814. <https://doi.org/10.1084/jem.20031454>.
- Wijenayaka AR, Kogawa M, Lim HP, Bonewald LF, Findlay DM, Atkins GJ. Sclerostin stimulates osteocyte support of osteoclast activity by a RANKL-dependent pathway. *Plos One.* 2011;6:9. <https://doi.org/10.1371/journal.pone.0025900>.

51. Shu R, Bai D, Sheu T, He Y, Yang X, Xue C, et al. Sclerostin promotes bone remodeling in the process of tooth movement. *PLoS One*. 2017;12, e0167312. <https://doi.org/10.1371/journal.pone.0167312>.
52. Atkins GJ, Rowe PS, Lim HP, Welldon KJ, Ormsby R, Wijenayaka AR, et al. Sclerostin is a locally acting regulator of late-osteoblast/preosteocyte differentiation and regulates mineralization through a MEPE-ASARM-dependent mechanism. *J Bone Min Res*. 2011;26:1425–1436. <https://doi.org/10.1002/jbmr.345>.
53. Twine NA, Chen L, Pang CN, Wilkins MR, Kassem M. Identification of differentiation-stage specific markers that define the ex vivo osteoblastic phenotype. *Bone*. 2014;67:23–32. <https://doi.org/10.1016/j.bone.2014.06.027>.
54. Otori F, Kitaura H, Marahleh A, Kishikawa A, Ogawa S, Qi J, et al. Effect of TNF-alpha-induced sclerostin on osteocytes during orthodontic tooth movement. *J Immunol Res*. 2019;2019, 9716758. <https://doi.org/10.1155/2019/9716758>.
55. Cawley KM, Bustamante-Gomez NC, Guha AG, MacLeod RS, Xiong J, Gubrij I, et al. Local production of osteoprotegerin by osteoblasts suppresses bone resorption. *Cell Rep*. 2020;32, 108052. <https://doi.org/10.1016/j.celrep.2020.108052>.
56. Tsukasaki M, Asano T, Muro R, Huynh NC, Komatsu N, Okamoto K, et al. OPG production matters where it happened. *Cell Rep*. 2020;32, 108124. <https://doi.org/10.1016/j.celrep.2020.108124>.
57. Aoki S, Honma M, Kariya Y, Nakamichi Y, Ninomiya T, Takahashi N, et al. Function of OPG as a traffic regulator for RANKL is crucial for controlled osteoclastogenesis. *J Bone Min Res*. 2010;25:1907–1921. <https://doi.org/10.1002/jbmr.89>.
58. Ostrowski MC. A new role for OPG: putting RANKL in its place. *J Bone Min Res*. 2010;25:1905–1906. <https://doi.org/10.1002/jbmr.206>.